# Supplementary material for Spatial characterization of long-term hydrological change in the Arkavathy watershed adjacent to Bangalore, India

## 1 Landsat imagery

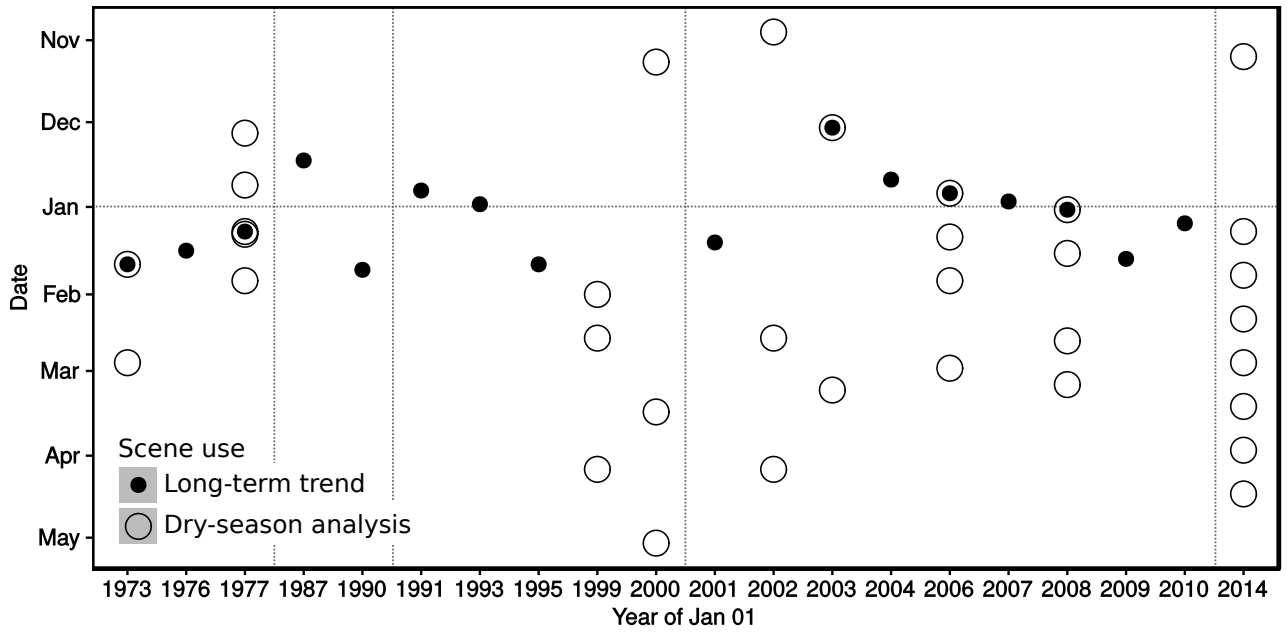


Figure 1: Landsat scenes analyzed in this study (N = 45), with the year corresponding to the date on January 1. Decades are separated by dashed vertical lines using "monsoon year" (e.g., the January 1990 image is grouped with the 1980s because it corresponds to the 1989 monsoon year).

| Date | Mission | Sensor | Path | Row | Cloud Free | Source | Use |
|---|---|---|---|---|---|---|---|
| 1973 January 22 | Landsat 1 | MSS | 154 | 051 | Yes | USGS | LTT,DSA |
| 1973 February 27 | Landsat 1 | MSS | 154 | 051 | Yes | USGS | DSA |
| 1976 January 17 | Landsat 2 | MSS | 155 | 051 | Yes | USGS | LTT |
| 1976 December 05 | Landsat 2 | MSS | 154 | 051 | | USGS | DSA |
| 1976 December 24 | Landsat 2 | MSS | 155 | 051 | Yes | USGS | DSA |
| 1977 January 10 | Landsat 2 | MSS | 154 | 051 | Yes | USGS | LTT,DSA |
| 1977 January 11 | Landsat 2 | MSS | 155 | 051 | Yes | USGS | DSA |
| 1977 January 28 | Landsat 2 | MSS | 154 | 051 | Yes | USGS | DSA |
| 1986 December 15 | Landsat 5 | TM | 144 | 051 | Yes | NRSC | LTT |
| 1990 January 24 | Landsat 5 | TM | 144 | 051 | Yes | NRSC | LTT |

Continued on next page

| Date | Mission | Sensor | Path | Row | Cloud Free | Source | Use |
|---|---|---|---|---|---|---|---|
| 1990 December 26 | Landsat 5 | TM | 144 | 051 | | NRSC | LTT |
| 1992 December 31 | Landsat 5 | TM | 144 | 051 | Yes | NRSC | LTT |
| 1995 January 22 | Landsat 5 | TM | 144 | 051 | Yes | NRSC | LTT |
| 1999 February 02 | Landsat 5 | TM | 144 | 051 | Yes | USGS | DSA |
| 1999 February 18 | Landsat 5 | TM | 144 | 051 | Yes | USGS | DSA |
| 1999 April 07 | Landsat 5 | TM | 144 | 051 | Yes | USGS | DSA |
| 1999 November 09 | Landsat 7 | ETM+ | 144 | 051 | Yes | USGS | DSA |
| 2000 March 16 | Landsat 7 | ETM+ | 144 | 051 | Yes | USGS | DSA |
| 2000 May 03 | Landsat 7 | ETM+ | 144 | 051 | | USGS | DSA |
| 2001 January 14 | Landsat 7 | ETM+ | 144 | 051 | Yes | USGS | LTT |
| 2001 October 29 | Landsat 7 | ETM+ | 144 | 051 | | USGS | DSA |
| 2002 February 18 | Landsat 7 | ETM+ | 144 | 051 | Yes | USGS | DSA |
| 2002 April 07 | Landsat 7 | ETM+ | 144 | 051 | | USGS | DSA |
| 2002 December 03 | Landsat 7 | ETM+ | 144 | 051 | Yes | USGS | LTT,DSA |
| 2003 March 09 | Landsat 7 | ETM+ | 144 | 051 | Yes | USGS | DSA |
| 2003 December 22 | Landsat 7 | ETM+ | 144 | 051 | Yes | USGS | LTT |
| 2005 December 27 | Landsat 7 | ETM+ | 144 | 051 | | USGS | LTT,DSA |
| 2006 January 12 | Landsat 7 | ETM+ | 144 | 051 | Yes | USGS | DSA |
| 2006 January 28 | Landsat 7 | ETM+ | 144 | 051 | | USGS | DSA |
| 2006 March 01 | Landsat 7 | ETM+ | 144 | 051 | | USGS | DSA |
| 2006 December 30 | Landsat 7 | ETM+ | 144 | 051 | Yes | USGS | LTT |
| 2008 January 02 | Landsat 7 | ETM+ | 144 | 051 | Yes | USGS | LTT,DSA |
| 2008 January 18 | Landsat 7 | ETM+ | 144 | 051 | Yes | USGS | DSA |
| 2008 February 19 | Landsat 7 | ETM+ | 144 | 051 | Yes | USGS | DSA |
| 2008 March 06 | Landsat 7 | ETM+ | 144 | 051 | Yes | USGS | DSA |
| 2009 January 20 | Landsat 7 | ETM+ | 144 | 051 | Yes | USGS | LTT |
| 2010 January 07 | Landsat 7 | ETM+ | 144 | 051 | | USGS | LTT |
| 2013 November 07 | Landsat 8 | OLI | 144 | 051 | | USGS | DSA |
| 2014 January 10 | Landsat 8 | OLI | 144 | 051 | | USGS | DSA |
| 2014 January 26 | Landsat 8 | OLI | 144 | 051 | Yes | USGS | DSA |
| 2014 February 11 | Landsat 8 | OLI | 144 | 051 | Yes | USGS | DSA |
| 2014 February 27 | Landsat 8 | OLI | 144 | 051 | | USGS | DSA,ACC |
| 2014 March 15 | Landsat 8 | OLI | 144 | 051 | Yes | USGS | DSA |
| 2014 March 31 | Landsat 8 | OLI | 144 | 051 | Yes | USGS | DSA |
| 2014 April 16 | Landsat 8 | OLI | 144 | 051 | | USGS | DSA |

Table 1: Landsat scenes analyzed. The path and row numbers refer to WRS-1 for Landsat 1–3 and WRS-2 for Landsat 5–8. "Use" column indicates whether the scene was used for calculation of long-term trends (LTT), dry-season analysis (DSA), or for accuracy assessment (ACC).

## 2 Classification flags

Figure 2: Left: Landsat false color composite (FCC) of a tank on 17 December 2005, with missing pixels visible as black diagonal bands. Middle: FCC after missing pixels were filled using successive grayscale dilation. Right: Classification of water in the image shown in blue.

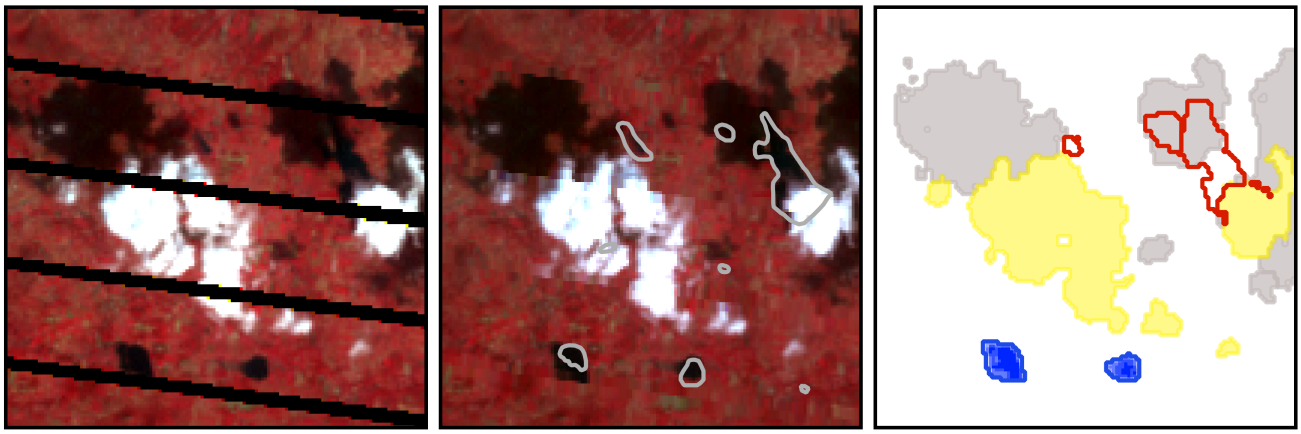

Figure 3: Left: Landsat false color composite on 27 December 2005 showing clouds and shadows near multiple tanks, with missing pixels visible as black diagonal bands. Middle: FCC after missing pixels were filled using successive grayscale dilation. Tank boundaries are shown in light gray. Right: Classification of clouds (yellow), cloud shadows (gray), water in tanks (blue), and areas classified as water but removed from the analysis due to clouds or cloud shadows (red outline).

# 3 Classification examples

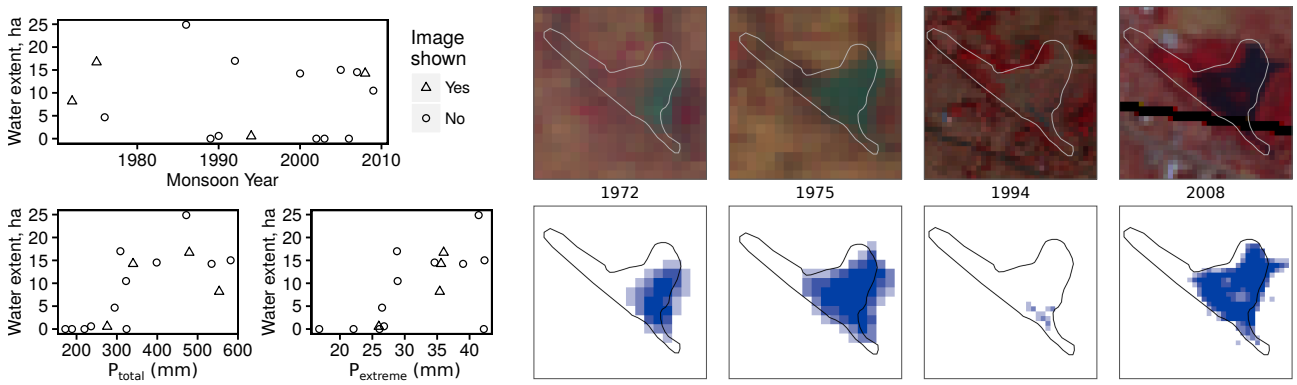


Figure 4: Left: Timeseries of tank water extent with selected Landsat images. Right: Landsat images (NIR-red-green mapped to red-green-blue) and corresponding classified water fraction.

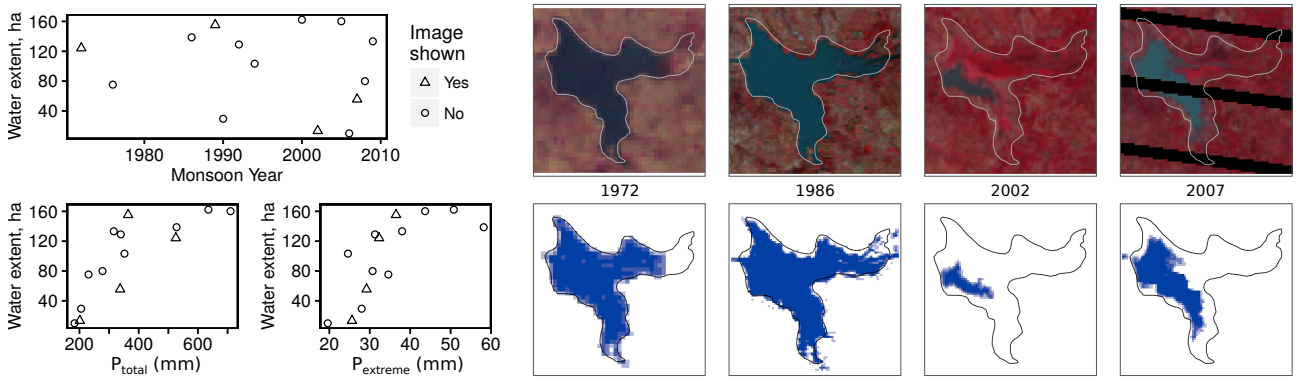


Figure 5: Left: Timeseries of tank water extent with selected Landsat images. Right: Landsat images (NIR-red-green mapped to red-green-blue) and corresponding classified water fraction.

# 4 Results from multiple regression

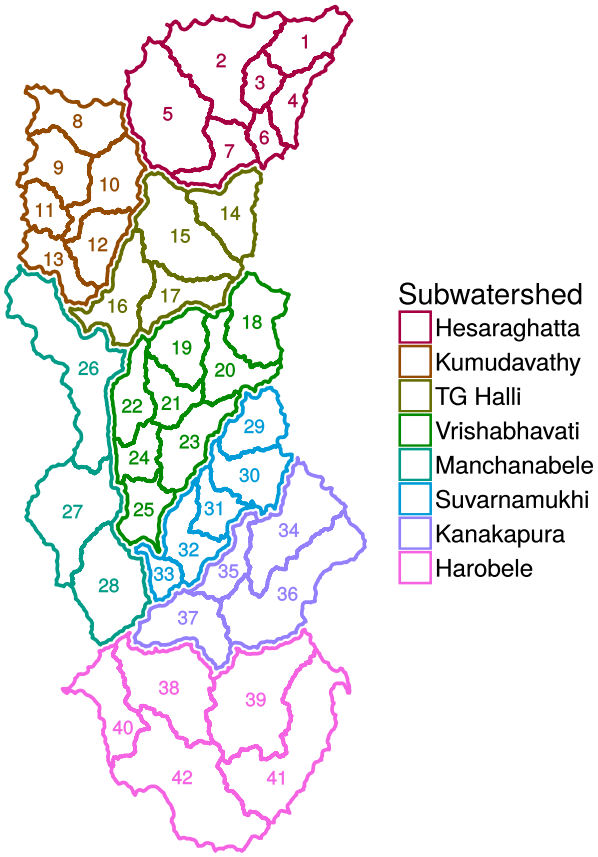


Figure 6: Subwatershed names and cluster IDs for the multiple regression. The Manchanabele and Harobele subwatersheds here are named for reservoirs within the watershed, which are not located at the subwatershed outlet.

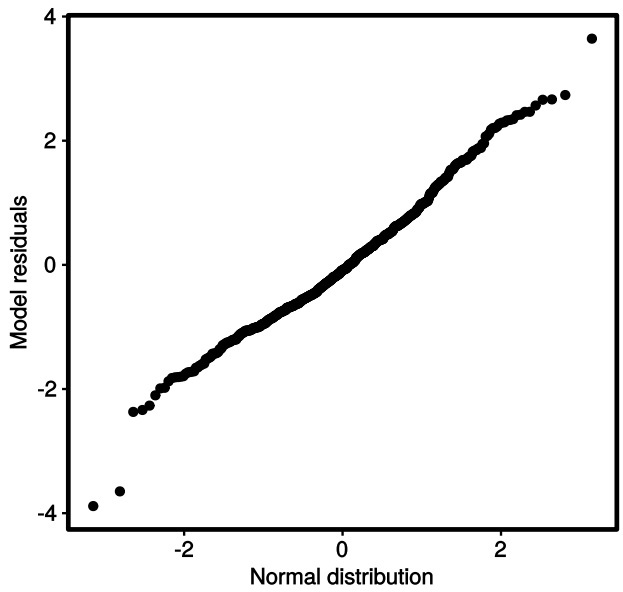


Figure 7: Quantile-quantile plot of residuals from multiple regression, with residuals normalized by mean and standard deviation and plotted agains a theoretical normal distribution.

| Variable | Watershed | Estimate | 95% Conf. Interval | Significant |
|---|---|---|---|---|
| P_total | Hesaraghatta | 0.0030 | [ 0.0011, 0.0048] | Y |
| P_total | Kumudavathy | 0.0048 | [ 0.0031, 0.0065] | Y |
| P_total | TG Halli | 0.0053 | [ 0.0032, 0.0073] | Y |
| P_total | Vrishabhavati | 0.0026 | [ 0.0013, 0.0040] | Y |
| P_total | Manchanabele | 0.0052 | [ 0.0031, 0.0074] | Y |
| P_total | Suvarnamukhi | 0.0029 | [ 0.0011, 0.0048] | Y |
| P_total | Kanakapura | 0.0027 | [ 0.0007, 0.0048] | Y |
| P_total | Harobele | 0.0037 | [ 0.0018, 0.0057] | Y |
| P_extreme | Hesaraghatta | 0.0824 | [ 0.0192, 0.1456] | Y |
| P_extreme | Kumudavathy | 0.0635 | [ 0.0065, 0.1206] | Y |
| P_extreme | TG Halli | 0.0563 | [ -0.0117, 0.1243] | |
| P_extreme | Vrishabhavati | 0.0960 | [ 0.0509, 0.1412] | Y |
| P_extreme | Manchanabele | 0.0345 | [ -0.0293, 0.0983] | |
| P_extreme | Suvarnamukhi | 0.0855 | [ 0.0277, 0.1433] | Y |
| P_extreme | Kanakapura | 0.0728 | [ 0.0025, 0.1431] | Y |
| P_extreme | Harobele | 0.0840 | [ 0.0295, 0.1385] | Y |
| L_dryseason | Hesaraghatta | -0.0062 | [ -0.0145, 0.0021] | |
| L_dryseason | Kumudavathy | -0.0187 | [ -0.0276,-0.0097] | Y |
| L_dryseason | TG Halli | -0.0169 | [ -0.0277,-0.0062] | Y |
| L_dryseason | Vrishabhavati | -0.0042 | [ -0.0119, 0.0034] | |
| L_dryseason | Manchanabele | 0.0046 | [ -0.0078, 0.0170] | |
| L_dryseason | Suvarnamukhi | -0.0023 | [ -0.0127, 0.0080] | |
| L_dryseason | Kanakapura | 0.0081 | [ -0.0033, 0.0196] | |
| L_dryseason | Harobele | -0.0021 | [ -0.0122, 0.0080] | |
| Trend | Cluster 1 | -8.5423 | [-13.1524,-3.9321] | Y |
| Trend | Cluster 2 | -5.7428 | [ -9.8688,-1.6168] | Y |

Continued on next page

| Variable | Watershed | Estimate | 95% Conf. Interval | Significant |
|---|---|---|---|---|
| Trend | Cluster 3 | -5.9023 | [ -9.2785,-2.5262] | Y |
| Trend | Cluster 4 | -6.0719 | [ -9.7290,-2.4149] | Y |
| Trend | Cluster 5 | -3.0386 | [ -6.3040, 0.2268] | |
| Trend | Cluster 6 | -4.9914 | [ -7.5963,-2.3865] | Y |
| Trend | Cluster 7 | -1.9311 | [ -3.2717,-0.5905] | Y |
| Trend | Cluster 8 | -6.0638 | [ -9.8431,-2.2845] | Y |
| Trend | Cluster 9 | -1.8920 | [ -4.3096, 0.5256] | |
| Trend | Cluster 10 | -0.6443 | [ -2.3368, 1.0483] | |
| Trend | Cluster 11 | -1.5497 | [ -3.0651,-0.0344] | Y |
| Trend | Cluster 12 | 0.5510 | [ -0.3884, 1.4904] | |
| Trend | Cluster 13 | 0.2430 | [ -0.4284, 0.9144] | |
| Trend | Cluster 14 | -2.4326 | [ -3.8343,-1.0309] | Y |
| Trend | Cluster 15 | -0.4811 | [ -1.8790, 0.9168] | |
| Trend | Cluster 16 | -0.0440 | [ -0.6246, 0.5367] | |
| Trend | Cluster 17 | 0.7534 | [ -0.4355, 1.9424] | |
| Trend | Cluster 18 | -0.1927 | [ -0.5592, 0.1737] | |
| Trend | Cluster 19 | 1.8104 | [ 0.1391, 3.4817] | Y |
| Trend | Cluster 20 | 1.3214 | [ 0.3053, 2.3374] | Y |
| Trend | Cluster 21 | 0.2823 | [ -1.0812, 1.6458] | |
| Trend | Cluster 22 | 0.2253 | [ -1.8224, 2.2730] | |
| Trend | Cluster 23 | 4.4629 | [ 1.3973, 7.5285] | Y |
| Trend | Cluster 24 | 0.3318 | [ -0.5243, 1.1879] | |
| Trend | Cluster 25 | -0.4928 | [ -1.6529, 0.6673] | |
| Trend | Cluster 26 | 0.0559 | [ -0.1662, 0.2779] | |
| Trend | Cluster 27 | -0.0627 | [ -0.5995, 0.4741] | |
| Trend | Cluster 28 | -0.5958 | [ -1.7350, 0.5433] | |
| Trend | Cluster 29 | 2.1627 | [ 0.9886, 3.3368] | Y |
| Trend | Cluster 30 | 0.5555 | [ -0.7622, 1.8732] | |
| Trend | Cluster 31 | 3.0785 | [ -0.4827, 6.6397] | |
| Trend | Cluster 32 | -0.1133 | [ -2.2537, 2.0270] | |
| Trend | Cluster 33 | 0.1548 | [ -0.6438, 0.9535] | |
| Trend | Cluster 34 | 0.6434 | [ -0.1912, 1.4780] | |
| Trend | Cluster 35 | -0.7273 | [ -2.2420, 0.7874] | |
| Trend | Cluster 36 | 0.0639 | [ -0.7680, 0.8957] | |
| Trend | Cluster 37 | -0.6639 | [ -2.5395, 1.2118] | |
| Trend | Cluster 38 | -0.0057 | [ -0.6712, 0.6598] | |
| Trend | Cluster 39 | 0.1250 | [ -0.2911, 0.5411] | |
| Trend | Cluster 40 | -1.7551 | [ -3.9551, 0.4450] | |
| Trend | Cluster 41 | -0.5841 | [ -1.6055, 0.4373] | |
| Trend | Cluster 42 | 0.1273 | [ -0.1511, 0.4058] | |

Table 2: Results from multiple regression for all varibles. The effects that apply at the subwatershed level are reported as directly output from the model. The temporal trend of each cluster was converted to units of ha per decade per 10 square km, matching Figure 8.

# 5 Dry-season analysis

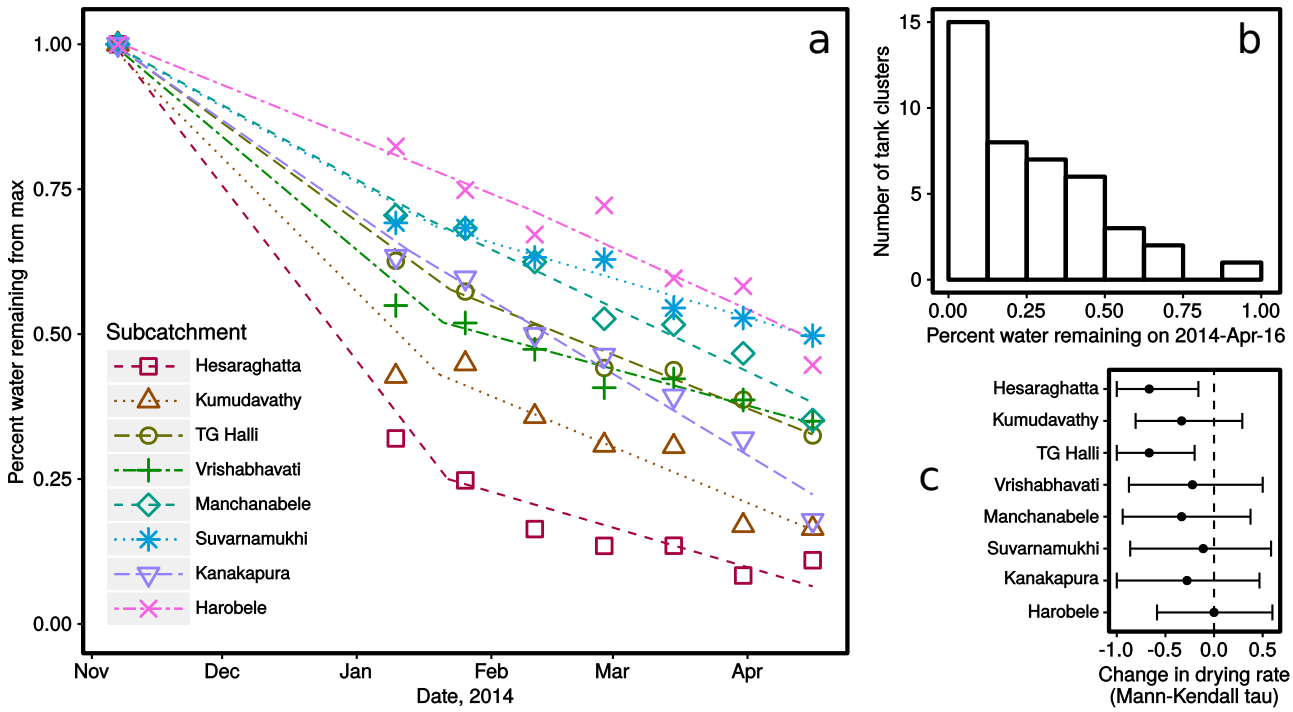


Figure 8: Dryseason analysis. (a) Post-monsoon drying of all tanks in each subwatershed, relative to the water extent at start of the dry season. The symbol for each subcatchment corresponds to the symbol in Figure 8 of Section 4.2 of the main article. (b) Histogram of the remaining water at the end of dry season as a fraction of the start of the dry season for all tank clusters. (c) Confidence intervals on the Mann–Kendall test statistic (tau) for a trend in the rate of tank water loss in dry season. Most subwatersheds do not exhibit a statistically significant trend in the rate of dry-season water loss (the confidence intervals include zero), but the Hesaraghatta and TG Halli subwatersheds exhibit a significant decreasing trend, meaning that tanks dry at a slower rate now than in the past.